

# Sprouty1 induces a senescence-associated secretory phenotype by regulating NF $\kappa$ B activity: implications for tumorigenesis

A Macià<sup>1,5</sup>, M Vaquero<sup>1,5</sup>, M Gou-Fàbregas<sup>1</sup>, E Castelblanco<sup>2</sup>, JM Valdivielso<sup>3</sup>, C Anerillas<sup>1</sup>, D Mauricio<sup>2,6</sup>, X Matias-Guiu<sup>4</sup>, J Ribera<sup>1</sup> and M Encinas<sup>\*,1</sup>

Genes of the Sprouty family (Spry1–4) are feedback inhibitors of receptor tyrosine kinase (RTK) signaling. As such, they restrain proliferation of many cell types and have been proposed as tumor-suppressor genes. Although their most widely accepted target is the Extracellular-regulated kinases (ERK) pathway, the mechanisms by which Spry proteins inhibit RTK signaling are poorly understood. In the present work, we describe a novel mechanism by which Spry1 restricts proliferation, independently of the ERK pathway. *In vivo* analysis of thyroid glands from Spry1 knockout mice reveals that Spry1 induces a senescence-associated secretory phenotype via activation of the NF $\kappa$ B pathway. Consistently, thyroids from Spry1 knockout mice are bigger and exhibit decreased markers of senescence including Ki67 labeling and senescence-associated  $\beta$ -galactosidase. Although such ‘escape’ from senescence is not sufficient to promote thyroid tumorigenesis in adult mice up to 5 months, the onset of Phosphatase and tensin homolog (Pten)-induced tumor formation is accelerated when Spry1 is concomitantly eliminated. Accordingly, we observe a reduction of SPRY1 levels in human thyroid malignancies when compared with non-tumoral tissue. We propose that Spry1 acts as a sensor of mitogenic activity that not only attenuates RTK signaling but also induces a cellular senescence response to avoid uncontrolled proliferation.

*Cell Death and Differentiation* (2014) 21, 333–343; doi:10.1038/cdd.2013.161; published online 22 November 2013

The Sprouty family of genes is composed of four members in mammals (*Spry1–4*), orthologous to a single *Drosophila melanogaster* gene (*dSpry*). With some well-documented exceptions, Sprouty proteins function as feedback inhibitors of receptor tyrosine kinase (RTK) signaling. In *Drosophila*, *dSpry* inhibits signaling by FGF and EGF in the airways and the eye, respectively. Genetic experiments in mice establish that Spry1 and Spry2 are negative regulators of signaling by FGFR and Ret RTKs. Thus, the deletion of Spry2 and/or Spry4 causes different craniofacial abnormalities because of hypersensitivity to FGF. On the other hand, excessive Ret signaling underlies kidney and enteric nervous system defects found in Spry1 and Spry2 knockout mice, respectively (reviewed in Guy *et al.*<sup>1</sup>). Although the most widely accepted targets of Spry are the ERK MAPK, the mechanisms by which Sprouty proteins restrain signaling by these RTKs remain poorly understood.<sup>1,2</sup>

Spry family members have been proposed to function as tumor-suppressor genes in a growing list of cancerous malignancies. Thus, Spry1 and Spry2 levels are decreased

in prostate and breast cancer,<sup>3,4</sup> whereas the downregulation of Spry2 has been described in hepatocellular carcinoma, B-cell lymphoma or endometrial carcinoma, among others.<sup>5–7</sup> Epigenetic silencing<sup>3,5</sup> or loss of heterozygosity<sup>3</sup> are the most widely observed molecular alterations of the *Spry* genes in tumoral tissue.

In this work, we show that Spry1 null mice exhibit overgrowth of the thyroid gland owing to increased proliferation of thyrocytes. Surprisingly, such increase in cell proliferation does not correlate with either elevation of systemic TSH levels or increased activation of the ERK MAPK pathway. Instead, thyroids from wild-type mice show markers of cellular senescence, which are absent in Spry1 knockout mice. More specifically, we found that Spry1 induces a senescence-associated secretory phenotype (SASP) by potentiating activation of the NF $\kappa$ B pathway. Moreover, deletion of Spry1 in the context of phosphatase and tensin homolog (Pten) haploinsufficiency results in increased incidence of tumors of the thyroid. In line with these data, expression levels of SPRY1 are reduced in human samples of thyroid cancer.

<sup>1</sup>Department of Experimental Medicine, Universitat de Lleida/Institut de Recerca Biomèdica de Lleida, Edifici Biomedicina I, Lab 2.8, Lleida 25198, Spain; <sup>2</sup>Department of Endocrinology, Universitat de Lleida/Institut de Recerca Biomèdica de Lleida, Lleida 25198, Spain; <sup>3</sup>Department of Experimental Nephrology, Universitat de Lleida/Institut de Recerca Biomèdica de Lleida, Lleida 25198, Spain and <sup>4</sup>Department of Pathology, Universitat de Lleida/Institut de Recerca Biomèdica de Lleida, Rovira Roure, 80, Lleida 25198, Spain

\*Corresponding author: M Encinas, Department of Experimental Medicine, Universitat de Lleida/Institut de Recerca Biomèdica de Lleida, Edifici Biomedicina I, Lab 2.8, Rovira Roure, 80, Lleida 25198, Spain. Tel/Fax: + 34 973702213; E-mail: mario.encinas@mex.udl.cat

<sup>5</sup>These authors contributed equally to this work.

<sup>6</sup>Present Address: Department of Endocrinology, University Hospital Germans Trias Pujol, 08916 Badalona, Spain.

**Keywords:** cellular senescence; tumor suppressors; sprouty; Pten; SASP; IL-6

**Abbreviations:** ERK, Extracellular-regulated kinases; MAPK, Mitogen-activated protein kinases; NF $\kappa$ B, Nuclear Factor  $\kappa$ B; TSH, Thyroid-stimulating hormone; Pten, Phosphatase and tensin homolog; STAT3, signal transducer and activator of transcription 3; IL-6, Interleukin-6

Received 25.7.13; revised 02.10.13; accepted 09.10.13; Edited by M Deshmukh; published online 22.11.2013

## Results

**Spry1 knockout mice have enlarged thyroid glands.** We have previously shown that Spry1 knockout mice exhibit thyroid C-cell hyperplasia.<sup>8</sup> While examining the number of C-cells, we noticed that thyroids from 3 months old Spry1 knockout mice, although having normal shape and showing no external signs of malignant growth, were bigger than those from wild-type littermates (Figure 1a). To confirm these observations, we estimated the thyroid lobe size from 3 months old wild-type and Spry1 null littermates. As shown in Figure 1b, thyroids from knockout mice were significantly larger than those from wild-type siblings. Such data were corroborated by measuring total RNA (Figure 1c) from thyroid homogenates. No differences on mouse weight were detected at this age, indicating that thyroid enlargement was specific (data not shown). At the histological level, thyroids from knockout mice were indistinguishable from those from wild-type littermates, showing no signs of neoplastic transformation (Figure 1e). Morphometric analyses revealed that an increase in follicle number but not size was responsible for their larger volume (Figures 1d and f). In conclusion, loss of Spry1 causes abnormal growth of the thyroid glands in the absence of morphologic signs of cellular transformation.

## Loss of Spry1 results in enhanced proliferation of follicular cells without affecting ERK phosphorylation.

We next assessed whether increased proliferation of follicular cells could account for the observed effects on thyroid size. Staining against Ki67 showed an increase in the number of positive cells in thyroids from null mice, indicating that thyrocyte proliferation is at least partially responsible for the observed phenotype (Figure 2a). Thyroid-stimulating hormone (TSH) is the master regulator of thyroid function and controls thyroid growth. No significant differences in serum levels of TSH were found between wild-type and Spry1 knockout mice (Figure 2b), indicating that increased systemic levels of TSH are not responsible for enlargement of the thyroid glands on mutant mice. On the other hand, circulating T3 and T4 levels were virtually identical between genotypes, indicating that thyroids from Spry1 knockout mice are euthyroid (Figures 2c and d). These data, together with high Spry1 levels found in mouse thyroid with respect to other organs,<sup>8</sup> suggested that Spry1 directly influences the proliferation of follicular cells in a cell-autonomous manner. To further support this notion, we isolated follicles from 3-month-old mice of both genotypes and found that follicular cells from mutant mice proliferated faster *in vitro*, as measured by 5'-bromo-deoxyuridine uptake (Figure 2f).

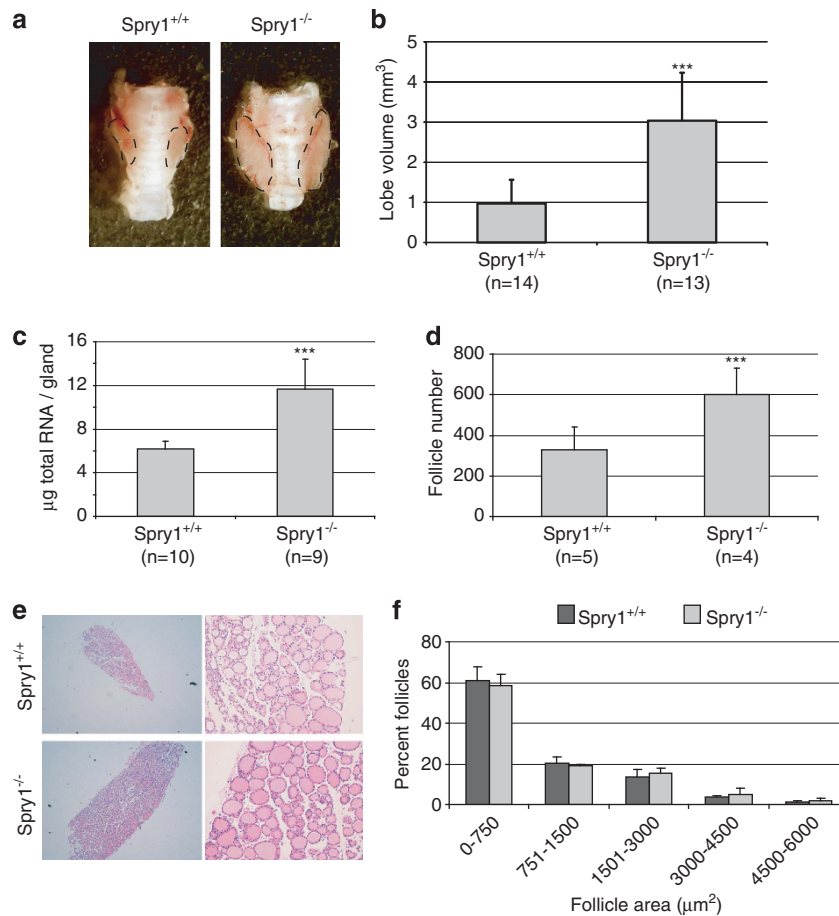


**Figure 1** Enlarged thyroid glands in Spry1 knockout mice. (a) Representative pictures of thyroid glands from the indicated genotypes. (b) Estimated lobe size, (c) mRNA contents and (d) follicle number of thyroid glands from wild-type and Spry1 knockout mice. (e) Hematoxylin–eosin staining of paraffin sections and (f) size–frequency histogram of follicles of thyroid glands from wild-type and Spry1 knockout. \*\*\* $P < 0.001$ , by two-tailed *t*-test

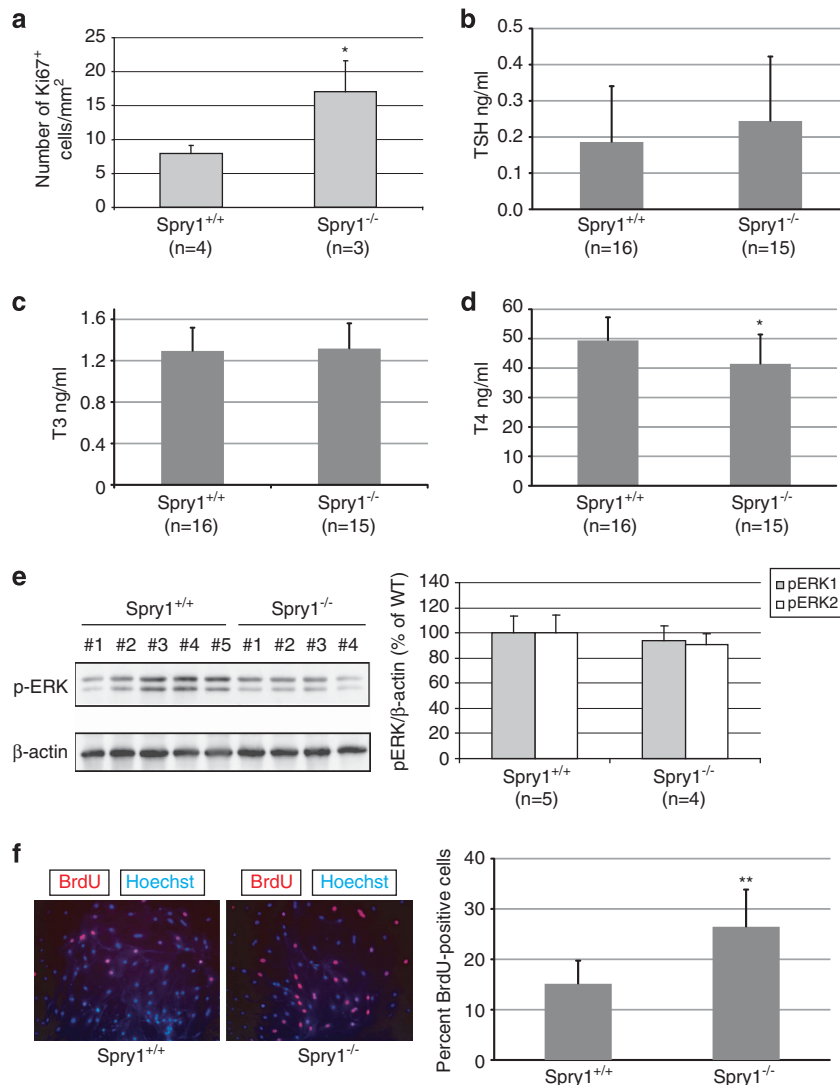


**Figure 2** Increased proliferation of thyroid follicular cells from Spry1 knockout mice. (a) Number of Ki67-positive cells on thyroid glands, and (b–d) serum TSH, T3 and T4 levels of 3-month-old wild-type and Spry1 knockout mice. (e) Genetic ablation of Spry1 does not induce hyperactivation of the ERK pathway. *In vivo* phosphorylation levels of ERK1/2 in the thyroid glands from both wild-type and Spry1 knockout mice. (f) Isolated follicular cells from knockout mice proliferate faster *in vitro*. \* $P < 0.05$  and \*\* $P < 0.01$ , by two-tailed *t*-test

As stated in the introduction, Sprouty proteins are regarded as inhibitors of the ERK MAP kinase pathway. Therefore, an attractive hypothesis to explain our observations could be that Spry1 null thyrocytes are more responsive to mitogens because of hyperactivation of the ERK pathway. We checked the status of the ERK pathway in thyroid follicular cells *in vivo* (Figure 2e, left panel) and to our surprise found no evidence of increased ERK phosphorylation in Spry1 null cells. Quantification of phospho-ERK levels with densitometry revealed no significant differences between wild-type and null mice and, if anything, showed a trend towards hypophosphorylation in null animals (Figure 2e, right panel). In conclusion, these data suggest that the overgrowth of the thyroid glands from knockout mice is not because of hyperactivation of the ERK pathway.

**Phosphorylation of STAT3 is eliminated in the thyroid from Spry1 knockout mice.** We then sought to investigate

whether the modification of signaling pathways other than ERK MAPKs could explain the observed phenotype. We monitored the activation status of the PI3-K/Akt, PLC $\gamma$ , Src and JAK-STAT pathways because they have been shown to be regulated by Sprouty family members in other systems. We also wanted to examine the Pten levels, as it has been reported that Spry2 exerts its inhibitory function via upregulation of Pten. As shown in Figure 3a, both phosphorylation of Akt and Pten levels were unchanged in the thyroids from knockout mice, whereas we could not detect phosphorylated PLC $\gamma$  or Src in either wild-type or mutant thyroids *in vivo*. However, we observed an almost complete ablation of phosphorylation of STAT3 at its activation residue (Tyrosine 705) in thyroids from Spry1 null animals (Figure 3a).

To establish whether such drastic reduction reflected an obligate role of Spry1 in STAT3 activation in the thyroid gland, we isolated follicles from both wild-type and null animals and stimulated them with its canonical activator,

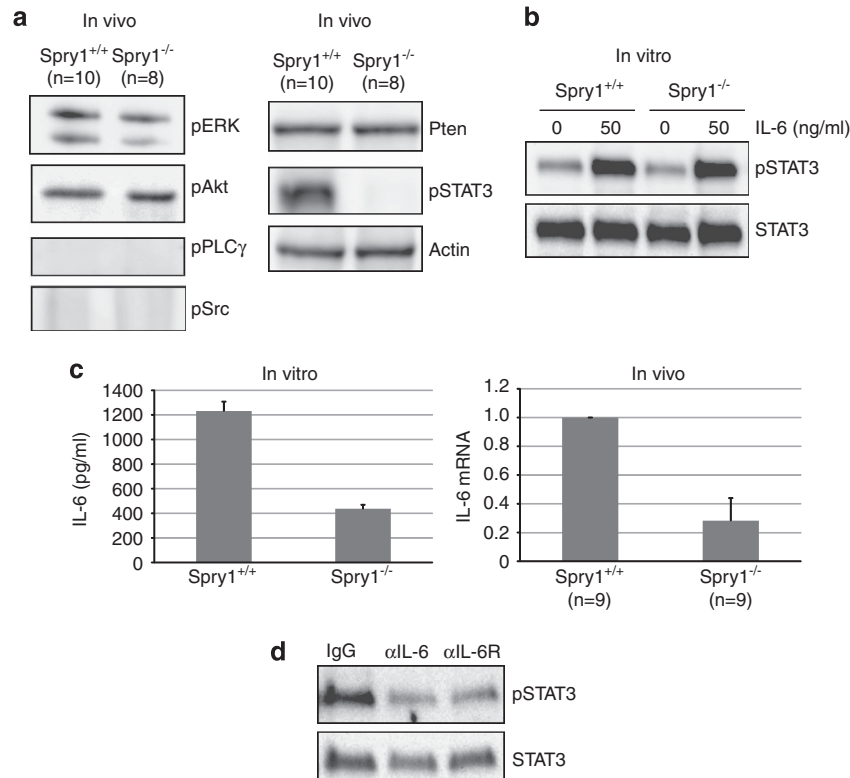


**Figure 3** Deletion of Spry1 disrupts an IL-6/STAT3 autocrine loop. (a) Immunoblot of the indicated (phospho) proteins from pooled samples of the indicated number of thyroid glands. (b) Phosphorylation of STAT3 upon the stimulation of isolated follicles with IL-6 (50 ng/ml, 5 min). (c) Left panel, IL-6 levels secreted by isolated follicles of the indicated genotypes as assessed using ELISA. Right panel, mRNA levels of IL-6 from pooled thyroids of the indicated genotypes. (d) Phospho-STAT3 levels of isolated follicles from wild-type mice incubated for 24 h with the indicated neutralizing antibodies

interleukin-6 (IL-6). Importantly, IL-6 is expressed in healthy human thyroid and is secreted by normal and transformed thyrocytes *in vitro*.<sup>9–11</sup> As shown in Figure 3b, stimulation with IL-6 induced a robust phosphorylation of STAT3 in cultured follicles from both wild-type and knockout mice, indicating that Spry1 is not necessary for STAT3 phosphorylation upon stimulation with IL-6. One possible explanation to these observations is that the loss of Spry1 results in decreased availability of STAT3 ligands rather than in reduced responsiveness to them. To assess this hypothesis, we measured IL-6 mRNA in whole thyroid glands from both genotypes and found a dramatic decrease in IL-6 levels in the thyroids from knockout mice (Figure 3c, right panel). To ascertain whether the source of IL-6 was follicular cells themselves, we isolated follicles from both the genotypes and assessed their ability to secrete IL-6 to the culture medium using ELISA. As shown in Figure 3c (left panel), thyroid follicular cells from wild-type mice secreted remarkable amounts of IL-6, which were drastically reduced in the case of Spry1<sup>-/-</sup> cells. Finally, to determine the contribution of IL-6 to STAT3 phosphorylation in thyrocytes, we incubated follicular cells from wild-type mice with neutralizing antibodies to IL-6 or IL6-R and assessed STAT3 phosphorylation. As shown in Figure 3d, blocking of either IL-6 or IL-6R greatly reduced STAT3 phosphorylation, suggesting that IL-6 is the major inducer of STAT3 phosphorylation in thyroid follicular cells. Taken together, these data indicate that the loss of Spry1 disrupts an autocrine IL-6/STAT3 loop in thyroid follicular cells.

**Thyroid follicular cells from Spry1 null mice show decreased markers of cellular senescence.** Cellular senescence is a state of growth arrest that can be triggered by either telomere attrition or by oncogenic stress (oncogene-induced senescence, OIS). A hallmark of senescent cells is the secretion of a set of cytokines and chemokines collectively known as Senescence-Associated Secretory Phenotype (SASP) or Senescence-Messaging Secretome (SMS) (reviewed in literature<sup>12–15</sup>). IL-6 and IL-8 are considered two of the most important cytokines secreted by senescent cells, which also secrete IGFBP7, IL-1 $\alpha$  or CXCL1, among others.<sup>16–19</sup> On the other hand, our previous results show that the overexpression of Spry1 in a medullary thyroid carcinoma cell line induces cellular senescence.<sup>8</sup> To explore the possibility that Spry1 induces cellular senescence in follicular cells via induction of an SASP, we collected supernatants from isolated follicles from wild-type and knockout thyroids and measured 62 different cytokines and chemokines using an antibody array (Figure 4a). Levels of IL-6, KC (CXCL1), MIPs, RANTES or sTNFR2, which are prominent SASP factors,<sup>15</sup> were severely reduced in supernatants from knockout cells, whereas IL-1 $\alpha$  was not. Other proteins present in the antibody array and involved in SASP such as IGFBP3, 5 or 6 were not detected (for a complete list of the cytokines analyzed see Supplementary Figure 1). On the other hand, mRNA levels of IGFBP7 were also reduced in mutant cells (Figure 4b, left panel). KC (also known as CXCL1 or GRO- $\alpha$  in humans) is thought to be one of the

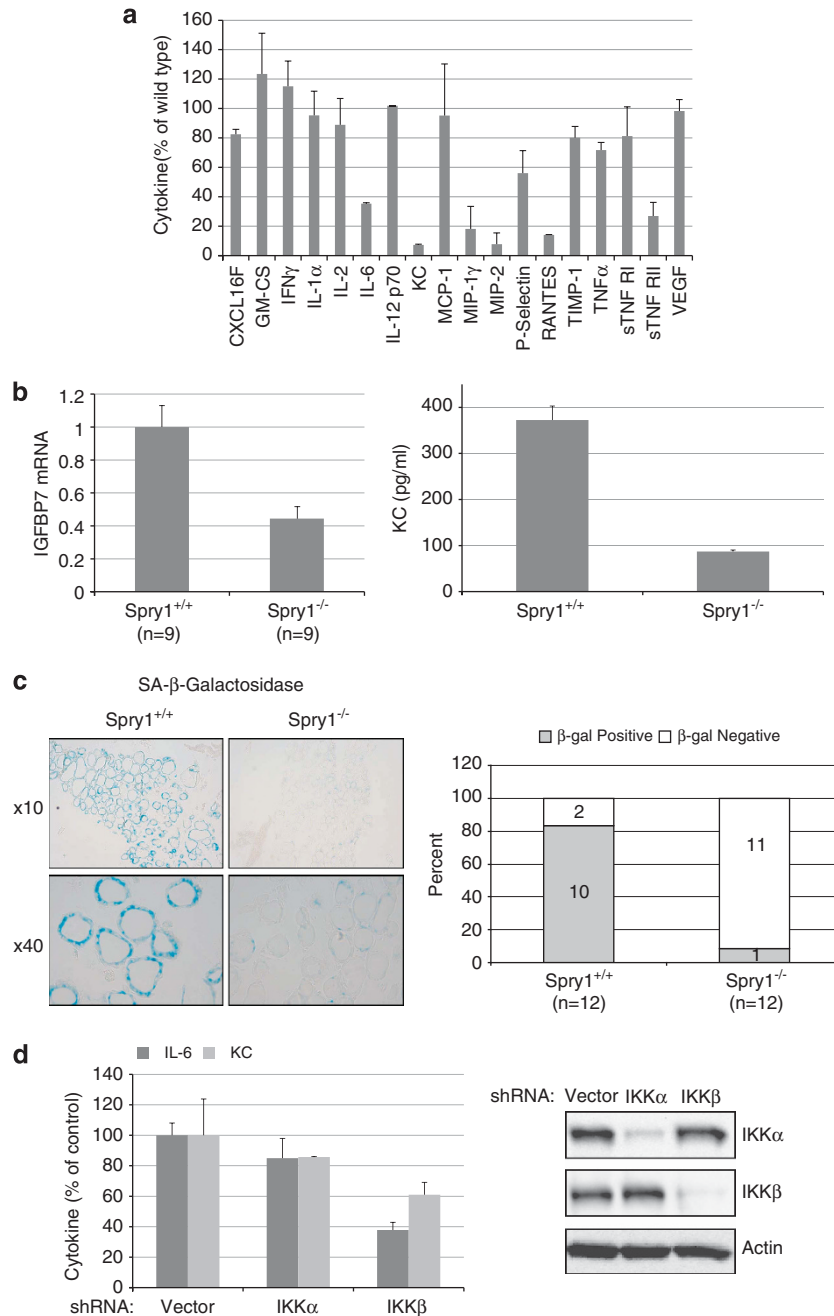


**Figure 4** Thyroid glands from Spry1 knockout mice exhibit decreased markers of cellular senescence. (a) Cytokine secretion profile of isolated follicles from knockout mice (100% is secretion of wild-type follicles). (b) Left panel, mRNA levels of IGFBP7 from pooled samples of the indicated number of thyroid glands and, right panel, KC levels secreted by isolated follicles of the indicated genotypes. (c) Senescence-associated beta galactosidase activity of wild-type versus Spry1 null thyroids. (d) Silencing of IKK $\beta$  reduces the secretion of both IL-6 and KC

functional homologs of the human *IL-8* gene, which is deleted in rodents. As both IL-8 and KC signal through the CXCR2 receptor, critical for the induction of senescence,<sup>16,20</sup> we confirmed the reduction in secreted KC by means of ELISA (Figure 4b, right panel). Moreover, we assayed senescence-associated  $\beta$ -galactosidase (SA- $\beta$ -Gal), the most widely used marker of cellular senescence, in frozen thyroid sections from wild-type and null 3-month-old mice. As shown in Figure 4c, virtually all follicular cells from wild-type mice were strongly positive for SA- $\beta$ -Gal activity, whereas only a

minority of cells from knockout mice was faintly stained. These observations, together with increased Ki67 labeling of knockout follicular cells and increased proliferation *in vitro*, suggest that these cells bypass a program of cellular senescence engaged in the normal thyroid glands.

**Activation of the NF $\kappa$ B pathway is impaired in Spry1<sup>-/-</sup> follicular cells.** IL-1 $\alpha$  has been shown to regulate the secretion of IL-6 and IL-8 in human senescent cells.<sup>21</sup> The observation that levels of IL1- $\alpha$  were similar in

supernatants from wild-type and knockout cells raised the possibility that Spry1 regulates generation of the SASP downstream of IL1- $\alpha$ . To test this hypothesis, we incubated isolated follicles from wild-type cells with IL-1 $\alpha$  and confirmed that this cytokine induces a robust secretion of both IL-6 and KC (Supplementary Figure 2). IL-1- $\alpha$  is a potent inducer of the NF $\kappa$ B pathway, which together with C/EBP $\beta$ , is critical for synthesis of the SASP factors.<sup>17,20–24</sup> We confirmed such a role of NF $\kappa$ B in our system by silencing either IKK $\alpha$  or IKK $\beta$  and measuring IL-6 and KC levels (Figure 4d). Whereas silencing of IKK $\alpha$  had only a modest influence on cytokine secretion, the effect of knocking down IKK $\beta$  was more profound, as expected for a role of the canonical NF $\kappa$ B

pathway on cytokine synthesis. To directly test whether activation of the NF $\kappa$ B pathway is compromised in the thyroids from Spry1 knockout mice, we first checked subcellular localization of p65, the major NF $\kappa$ B subunit that accumulates on the chromatin of senescent cells<sup>22</sup> and found that it was mostly excluded from the nucleus of follicular cells from knockout but not wild-type mice (Figure 5a). Accordingly, levels of I $\kappa$ B $\alpha$ , which is responsible for retention of NF $\kappa$ B dimers in the cytoplasm, were increased in the knockout thyroid (Figure 5b). Moreover, nuclear translocation of p65 upon LPS injection was diminished, although not completely prevented in thyroid tissue from mutant mice (Figures 5c and d). Accordingly, although I $\kappa$ B $\alpha$  degradation

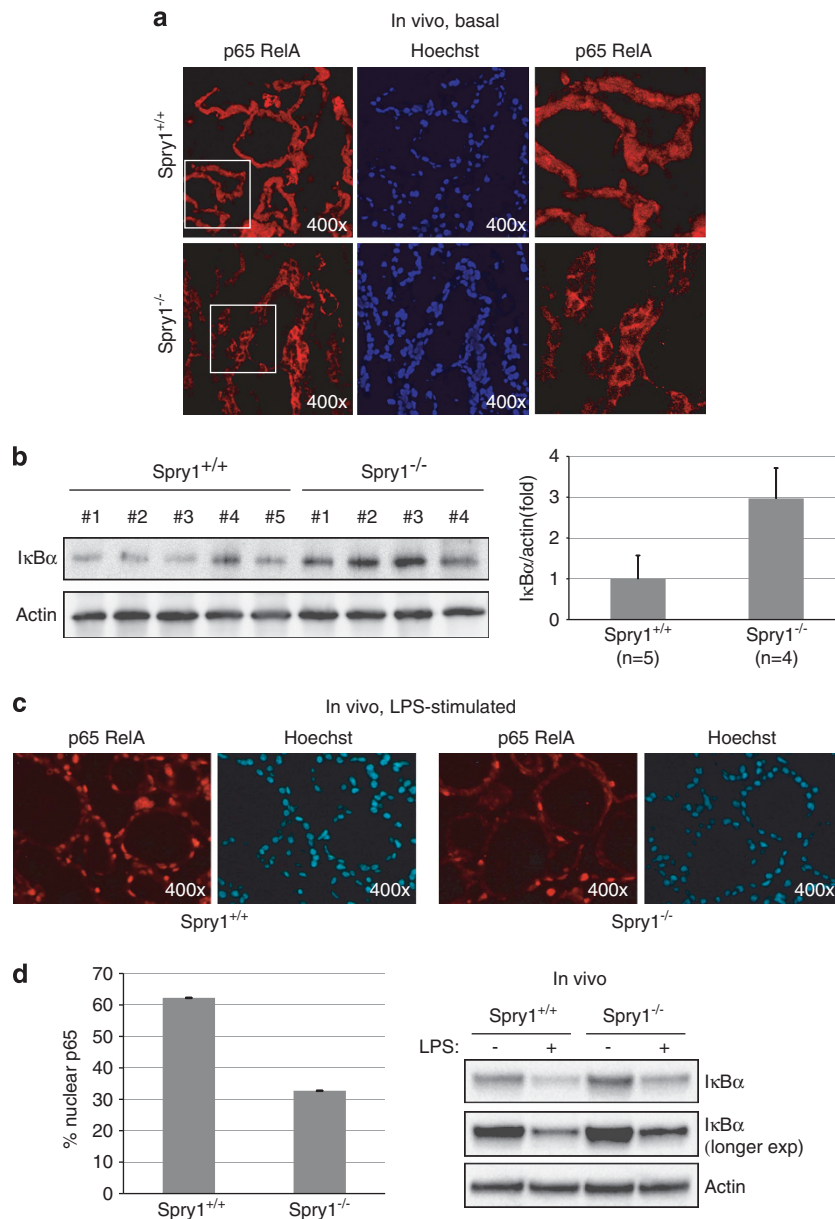


**Figure 5** Activation of the NF $\kappa$ B pathway is compromised in thyroids from Spry1 knockout mice. (a) Immunostaining against p65 on frozen sections of thyroids of the indicated genotypes. (b) Steady-state levels of I $\kappa$ B $\alpha$  of thyroids from 3-month-old mice of the indicated genotypes. (c) Immunostaining against p65 on frozen sections of thyroids of the indicated genotypes, stimulated with LPS. (d) Left panel, nuclear translocation of p65 after stimulation with LPS. Right panel, I $\kappa$ B $\alpha$  levels on thyroids from mice of the indicated genotypes injected with saline or LPS

was not impaired, I $\kappa$ B $\alpha$  levels after LPS challenging remained higher in thyroids from knockout mice when compared with wild-type mice (Figure 5d). Taken together, these data strongly suggest that follicular cells from Spry1 knockout mice are defective in NF $\kappa$ B activation and consequently fail to synthesize appropriate amounts of SASP factors.

**Genetic deletion of Sprouty1 accelerates pten-induced thyroid tumorigenesis.** OIS is regarded as a defense mechanism against tumoral transformation elicited by oncogenic insults. As such, cells lacking essential components of the cellular senescence machinery are more susceptible to tumoral transformation. To test whether thyroid cells from Spry1 knockout mice were prone to transformation upon oncogenic stimulation, we crossed Spry1-knockout mice to Pten heterozygous mice. We chose Pten-deficient mice for three main reasons: first, they develop a wide range of tumors including thyroid carcinoma;<sup>25–27</sup> second, Pten loss has been found to be a potent inducer of cellular senescence;<sup>28,29</sup> and third, STAT3 is tumor-suppressive in gliomas bearing Pten mutations.<sup>30</sup> Genetic ablation of Spry1 in the context of Pten haploinsufficiency resulted in the development of hyperplastic follicular lesions as early as 3 months of life, age at which thyroid glands from their

Pten<sup>+/-</sup> littermates were normal (Figure 6a). By 5 months of age, even though a fair percentage of Pten<sup>+/-</sup> mice presented nodular hyperplasia of the follicular cells, lesions in double-mutant mice were much larger (Figure 4b), and sometimes presented areas with normal follicles had been substituted by solid lesions consisting of large eosinophilic cells (Figure 6c). In regions where the follicular architecture was preserved, some follicles presented structures resembling small papillae, whereas some others were composed of tall cells (Figure 6c). Finally, thyroids from double-mutant mice strongly stained for the proliferation marker Ki67 (Figure 6d). In conclusion, although loss of Spry1 by itself was not enough to promote transformation of the thyroid tissue, when combined with Pten haploinsufficiency it greatly accelerated the appearance of neoplastic growth of the thyroid.

**Decreased levels of Spry1 and IL-6 in human thyroid adenomas and follicular carcinomas.** To begin to elucidate whether our findings could be relevant to human pathology, we analyzed the expression of SPRY1 on a series of 14 thyroid follicular adenomas and carcinomas (nine adenomas and five carcinomas) and 10 non-matched, non-tumoral adjacent thyroid samples (Supplementary Figure 3). The median expression of SPRY1 was significantly

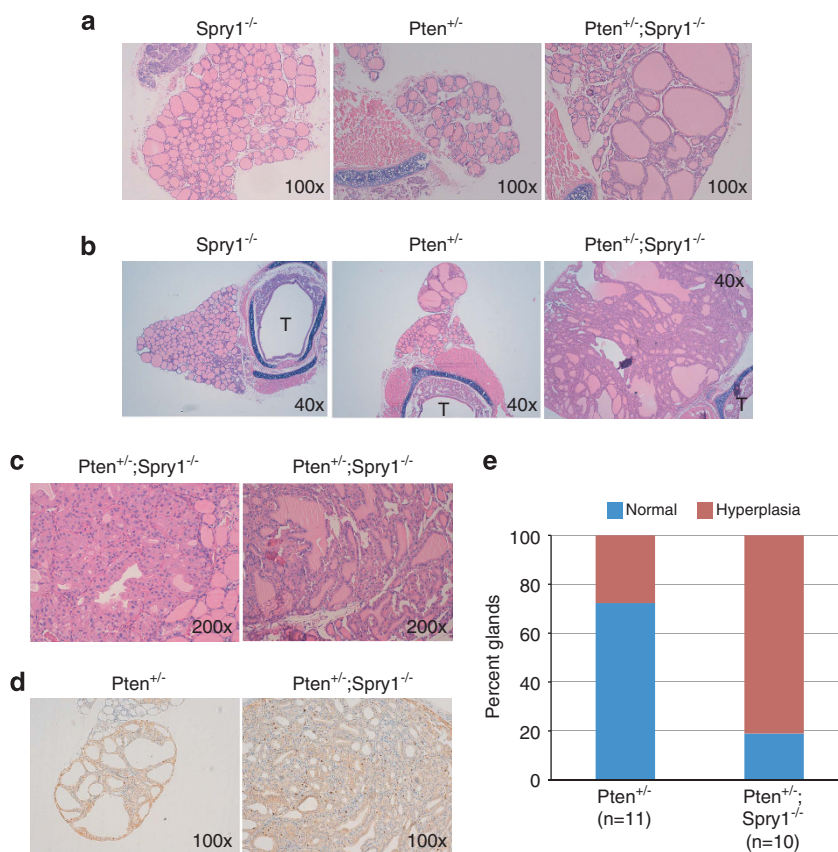


**Figure 6** Loss of Spry1 accelerates thyroid tumorigenesis in the context of Pten haploinsufficiency. (a) Hematoxylin–eosin staining of thyroid glands from 3-month-old animals of the indicated genotypes. (b) Same for 5-month-old animals. T, trachea. (c) Higher magnification of thyroids from double-mutant mice. (d) Ki67 labeling of thyroids from 5-month-old mice of the indicated genotypes. (e) Stack bar graph showing the effect of loss of Spry1 in thyroids from 3- to 5-month-old animals

reduced in tumor samples when compared with non-tumoral tissue (Man–Whitney's *U*-test;  $P=0.017$ ). Moreover, consistent with our findings, levels of IL-6 mRNA were also significantly decreased in tumors versus normal samples (Man–Whitney's *U*-test;  $P=0.002$ ; Figure 7b). Univariate regression analysis showed that Sprouty expression was significantly associated with IL-6 levels ( $\beta$ : 1.072; CI 95%: 0.63–1.514;  $P<0.001$ ;  $R^2$ : 0.576, Figure 7c). Finally, hematoxylin–eosin staining of normal tissue did not show any signs of infiltration, ruling out a misleading effect of immune cells on levels of IL-6 (Figure 7d). Taken together, these findings suggest that SPRY1 may have a role as a tumor suppressor in thyroid follicular carcinoma.

## Discussion

In the present work, we have unveiled a new role of Spry1 in inducing cellular senescence, independently of the ERK pathway, the most widely accepted target of Spry proteins. We found that loss of Spry1 disrupts an autocrine loop by reducing IL-6 synthesis and subsequent STAT3 phosphorylation. STAT3 is a pleiotropic transcription factor that influences proliferation, differentiation and survival of multiple cell types. It can induce proliferation by promoting expression of its transcriptional targets Cyclin D or c-Myc, but paradoxically, STAT3 activation is cytostatic in other cell types via the induction of cell cycle inhibitors such as p21<sup>CIP</sup>, p27<sup>KIP</sup> or p14<sup>Arf</sup> (reviewed in Bowman *et al.*<sup>31</sup> and Smithgall *et al.*<sup>32</sup>). This dual mode of action is perhaps best illustrated by the opposing effects of activated STAT3 on tumorigenesis. Thus, after being identified as an oncogene in some cancer

types,<sup>31,33</sup> recent work has highlighted its role as tumor suppressor in glioma, hepatoma, breast, intestinal, head and neck and thyroid cancer.<sup>11,30,34–38</sup> Interestingly, Couth *et al.*<sup>11</sup> found that an autocrine IL6/gp130/JAK loop is responsible for keeping high levels of phospho-STAT3 phosphorylation in thyroid carcinoma cell lines, which in turn suppress tumorigenesis.

Although our results could, therefore, be explained on the basis of such autocrine loop and its effect on STAT3 phosphorylation, we found that Spry1-deficient cells are defective on the secretion of not only IL-6 but a series of factors that belong to the SASP. Whereas some of these factors can induce proliferative responses in a paracrine manner,<sup>15</sup> it is now clear that at least some others, namely IL-6, IL-8 and IGFBP7, have a causal role in the induction and maintenance of both replicative and OIS, in an autocrine manner.<sup>16,17,19</sup> It is now well established that senescent cells normally persist in the adult organism – for example, in benign or pre-malignant lesions such as moles<sup>39</sup> – but also in normal tissue.<sup>40–42</sup> It should be noted that the thyroid gland is considered to be a dormant, non-regenerative organ with very slow cellular turnover: in humans, it has been estimated that follicular cells divide approximately five times during adult life.<sup>43</sup>

A growing number of evidence links activation of the NF $\kappa$ B pathway to induction of the SASP and cellular senescence,<sup>24,44,45</sup> and indeed CHIP experiments demonstrate that p65 is the most abundant transcription factor bound to senescent chromatin.<sup>22</sup> As for the mechanism by which Spry1 modulates the NF $\kappa$ B pathway, the lack of a universal mode of action of Spry proteins makes it difficult to explore candidate

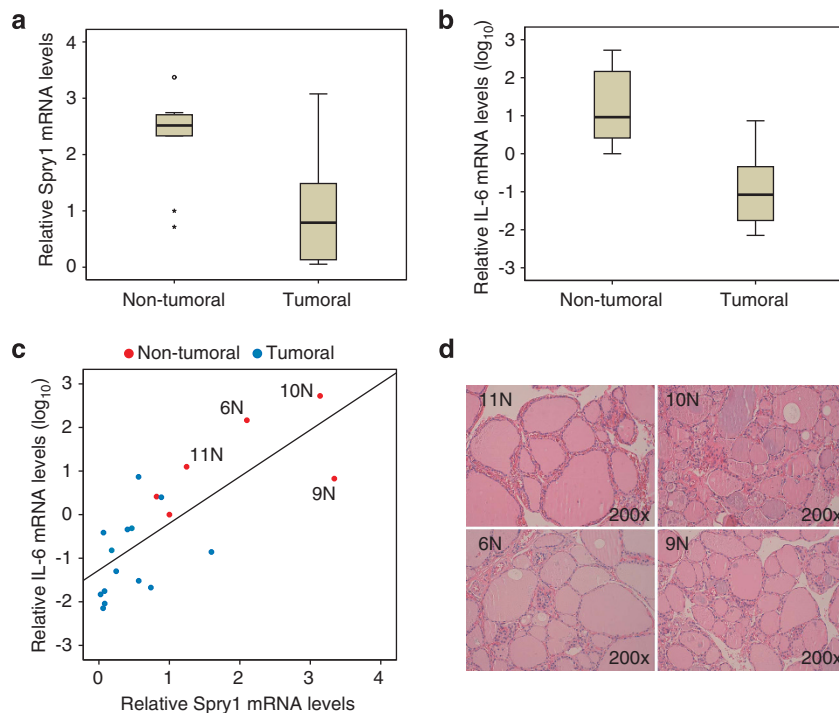


**Figure 7** SPRY1 and IL-6 levels are reduced in human thyroid tumors. (a) Relative SPRY1 mRNA levels of non-tumoral versus tumoral thyroid tissue. ( $P<0.05$  by Man–Whitney's *U*test). (b) Relative IL-6 mRNA levels of non-tumoral versus tumoral thyroid tissue. ( $P<0.01$  by Man–Whitney's *U*-test). (c) Scatter plot of IL-6 versus SPRY1 levels. (d) Hematoxylin–eosin staining of normal thyroid tissue of the indicated samples (selected because of their higher levels of IL-6) shows no evidence of infiltration



pathways. Owing to the absence of true conserved domains in Spry proteins, one strategy to investigate its mechanism of action has been to identify their binding partners, in a 'guilty-by-association' approach.<sup>1</sup> Following this reasoning, we envisage several potential mechanisms by which Spry1 could modulate the pathway. For example, dendritic cells lacking c-Cbl, a well-known Spry-binding partner, show increased cytokine secretion owing to augmented NF $\kappa$ B activity.<sup>46</sup> On the other hand, the adaptor protein CIN85, which also interacts with Spry1/2, is necessary for activation of the NF $\kappa$ B pathway in B lymphocytes upon BCR stimulation.<sup>47</sup> Finally, kinases of the Raf family including B-Raf interact with Spry1,<sup>1</sup> and Raf activation has been mechanistically linked to activation of the NF $\kappa$ B pathway.<sup>48</sup> In conclusion, there are many potential mechanisms by which Spry1 can induce NF $\kappa$ B activity that deserve further investigation. In this regard, our preliminary data indicate that overexpression of Spry1 in 293 cells enhances NF $\kappa$ B activity in luciferase assays (data not shown). The use of systems more suitable for manipulation such as 293 cells should allow us to investigate these mechanisms in more depth.

Besides induction of SASP via NF $\kappa$ B activation, we cannot rule out the existence of other mechanisms by which Spry1 expression induces cellular senescence. For instance, it has been shown that Spry1 binds to the adenoviral protein E1A,<sup>49</sup> whose ability to promote evasion of Ras-induced senescence has been repeatedly reported. On the other hand, a recent report describes that the kinase Dyrk1A, a well-known interactor of Spry proteins,<sup>1,2</sup> promotes cellular senescence via the phosphorylation of LIN52 and assembly of the DREAM transcriptional repressor.<sup>50</sup>

To conclude, we have also shown that deletion of Spry1 accelerates the onset of thyroid tumorigenesis in Pten<sup>+/-</sup> mice. These data are in agreement with two recent reports showing that deletion of Spry family members in the context of Pten haploinsufficiency accelerates prostate tumorigenesis.<sup>51,52</sup> During the last years, it is becoming evident that OIS poses a potent barrier to tumoral transformation *in vivo*. Thus, the expression of activated Ras, E2f3 or B-Raf oncogenes in mice induces cellular senescence in premalignant tumors of the lung, pancreas, mammary gland, pituitary gland and melanoma. The loss of senescence responses induced by genetic ablation of Cdkn2a or Trp53 leads to malignant progression of these tumors (reviewed in Priuer and Peepers<sup>53</sup> and Collado and Serrano<sup>54</sup>). Similarly, conditional deletion of Pten in the prostate induces cellular senescence that is bypassed by concomitant deletion of Trp53.<sup>28</sup> Importantly, bypass of OIS and subsequent tumor progression can also be achieved by the removal of SASP factors or their receptors in colon adenoma, prostate carcinoma or melanoma.<sup>17,19,20</sup>

We have finally found that human thyroid follicular adenomas and carcinomas show decreased levels of SPRY1 and IL-6 with respect to normal tissue. Consistent with our data, a reduction in IL-6 levels has been reported both in well-differentiated thyroid carcinomas with respect to normal tissue, which becomes more evident as tumors progress to undifferentiated thyroid carcinoma.<sup>55</sup> Moreover, recent evidence points to an important role of IGFBP7 and OIS in the suppression of thyroid carcinoma.<sup>56</sup> Finally, promoters of both

SPRY1 and SPRY2 have been found to be differentially methylated in tumoral versus normal thyroid tissue.<sup>57</sup>

In conclusion, we have found that Spry1 controls the transition of thyrocytes to a state of cellular senescence by regulating the appearance of SASP. Interestingly, a recent report shows that negative feedback mechanisms (including expression of Spry1) in response to activation of the Ras/Raf/ERK pathway are indeed responsible for the senescence response.<sup>58</sup> Thus, one interesting concept would be that Spry proteins sense mitogenic activity and respond not only by attenuating signaling pathways triggered by mitogens but also by inducing a senescence response to avoid uncontrolled proliferation.

#### Materials and Methods

**Ethics statement.** All experimental procedures involving animals were in accordance with the national and regional guidelines and were approved by the Experimental Animal Ethic Committee of the University of Lleida. Studies using human samples were approved by the Ethics Committee on Clinical Investigation of the Hospital Universitari Arnau de Vilanova, and all patients gave their informed consent.

**Mice.** Mice knockout for Spry1 were a generous gift of Dr. M Albert Basson (King's College, London, UK). Heterozygous mice for Pten were obtained from the NCI mouse repository at <http://mouse.ncicrf.gov/>. All mice were maintained on a 129/Sv  $\times$  C57/BL6 mixed background. When indicated, mice were injected *i.p.* with 75  $\mu$ g of lipopolysaccharide (Sigma, St. Louis, MO, USA) or PBS as control for 1 h.

**Morphometric analysis.** Estimation of thyroid gland size was performed by using the ellipsoid formula (width  $\times$  height  $\times$  depth  $\times$   $\pi/6$ ). Thyroid follicle number and area were scored on hematoxylin–eosin-stained sections using the Cell Profiler software (<http://www.cellprofiler.org>). Nuclear p65 was automatically scored using the ImageJ software (Bethesda, MD, USA) (find maxima process, set to noise tolerance 12).

**Hormone measurement.** Serum levels of T3, T4 and TSH were measured using the MilliplexMAP Rat thyroid kit (Millipore, Bedford, MA, USA) according to the manufacturer's instructions. The kit reacts with both rat and mouse T3 and T4 but is intended for determination of rat TSH. However, others have shown that it is suitable for determination of relative levels of murine TSH.<sup>59</sup>

**Western blot.** Western blot was conducted as described.<sup>60</sup> Immunoblots were developed using a VersaDoc device (Bio-Rad, Hercules, CA, USA), and densitometry was performed using its software package (ImageLab, Bio-Rad). Antibodies used are detailed in Supplementary Figure 4.

**ELISA and antibody array.** ELISA for IL-6 was performed using the RayBiotech (Norcross, GA, USA) Mouse IL-6 ELISA kit according to the manufacturer's instructions. For determination of KC, we used the Murine KC Mini ELISA Development Kit from Peprotech (Rocky Hill, NJ, USA). For determination of multiple cytokines in cell supernatants, we used the RayBio Mouse Cytokine Antibody Array G-Series 3 (no. AAM-CYT-G3-4) as directed by the manufacturers. Slides were scanned using a GenePix 4000A laser scanner (Axon, Sunnyvale, CA, USA).

**Immunocytochemistry and immunofluorescence.** Immunocytochemistry against Ki67 was performed on paraffin sections. Briefly, sections were dewaxed and submitted to antigen retrieval (95 °C for 20 min in Tris/EDTA buffer, pH 9) using a PTLink apparatus (DAKO, Glostrup, Denmark). Staining was performed using an Autostainer device (DAKO) using biotinylated secondary antibodies and HRP-coupled streptavidin. Sections were counterstained with hematoxylin. For p65 immunofluorescence, frozen sections were permeabilized with 100% methanol blocked with goat serum and incubated overnight at 4 °C with primary antibody. Secondary antibody was incubated for 2 h at room temperature. Nuclear staining was obtained with Hoescht 33258. Antibodies used are detailed in Supplementary Figure 4.

**Isolation and culture of thyroid follicles.** Thyroid glands were excised from the indicated mice and digested in 1 mg/ml collagenase IV and 1.2 U/ml dispase II (both from Roche, Basel, Switzerland) in phosphate-buffered saline for 40 min at 37 °C. After trituration with a blue tip, follicles were allowed to settle by gravity and separated from single cells. Follicles were then washed and plated in complete medium containing FBS and TSH overnight, switched to serum-free media and supernatants were collected 24 h later. When indicated, blocking antibodies (Supplementary Figure 4) were added. Lentiviral infection and sequences of shRNAs used are described elsewhere.<sup>60</sup> For BrdU uptake experiments, follicles were isolated as above and cultured in complete medium for 48 h. Cells were pulsed with BrdU for the last 4 h, fixed and BrdU staining performed as described.<sup>8</sup>

**Real time RT-PCR.** Total RNA was extracted with a RNeasy Mini Kit (QIAGEN, Hilden, Germany). RNA was quantitated using a Nanodrop device. Taqman technology from Applied Biosystems (Warrington, UK) was used for real-time RT-PCR analyses. Probes included mouse IL-6 (Mm00446190\_m1), Igf1p7 (Mm03807886\_m1), Gapdh (Mm9999915\_g1), and human IL-6 (Hs00985639\_m1), SPRY1 (Hs00398096\_m1), and GAPDH (Hs99999905\_m1). Results were calculated by the  $2^{-\Delta\Delta C_t}$  method. Expression levels were normalized to GAPDH. For human tissue samples, levels of SPRY1 or IL-6 were expressed as fold change relative to RNA from healthy human thyroid obtained from a commercial source (Ambion, Grand Island, NY, USA), which was also included in the non-tumoral group.

**Senescence-associated  $\beta$ -galactosidase activity.** SA- $\beta$ -Gal staining of was carried out as described.<sup>8</sup> Briefly, paraformaldehyde-fixed frozen sections were incubated with X-gal solution (20 mg/ml X-Gal (Sigma), 5 mM  $K_3Fe(CN)_6$ , 5 mM  $K_4Fe(CN)_6$  and 2 mM  $MgCl_2$ ) in PBS at pH 6.0 during at least 2 h at 37 °C. To allow comparison between specimens, all samples were assayed simultaneously.

**Human tissue samples.** Frozen thyroid samples ( $n=23$ ) from unrelated patients were obtained from the Biobanc IRBLleida and RETIC Biobancos RD09/0076/00059. The samples consisted of five follicular thyroid carcinomas (FTC), nine follicular adenomas (AF) and nine normal thyroid samples (Supplementary Figure 3). Diagnoses were evaluated by pathologists using hematoxylin–eosin staining according to the World Health Organization (WHO) criteria and the frozen tissues were stored in O.C.T (VWR International) at  $-80$  °C before isolation of the DNA and RNA.

**Statistical analysis.** The Shapiro–Wilk test was used to determine whether variables followed a normal distribution. Data are presented as mean  $\pm$  S.D. for quantitative variables following a normal distribution or as medians when distributions were not normal. A Student's *t*-test was used to compare the means between normally distributed variables, whereas Man–Whitney's *U*-test was used otherwise. Univariate regression analysis was used to determine whether association was detected between two continuous variables.

### Conflict of Interest

The authors declare no conflict of interest.

**Acknowledgements.** We thank Lidia Parra, Cristina Girón, Sònia Gatiús and Maria Santacana for technical support. This work was supported by grants from Ministerio de Economía y Competitividad (BFU2007-67619 and BFU2010-17628) and Fundació La Marató de TV3 (101810), and funding from Suport als Grups de Recerca (2009 SGR 740) from Generalitat de Catalunya to ME, AM is supported by a predoctoral fellowship from Universitat de Lleida and was supported by a fellowship from a Fundació Alicia Cuello de Merigó. MV is supported by a predoctoral fellowship from AGAUR (Generalitat de Catalunya). MG-F is supported by a grant from Fundació La Marató de TV3. CA was supported in part by a Beca de Colaboración (MEC).

- Guy GR, Jackson RA, Yusoff P, Chow SY. Sprouty proteins: modified modulators, matchmakers or missing links? *J Endocrinol* 2009; **203**: 191–202.
- Edwin F, Anderson K, Ying C, Patel TB. Intermolecular interactions of Sprouty proteins and their implications in development and disease. *Mol Pharmacol* 2009; **76**: 679–691.

- McKie AB, Douglas DA, Olijslagers S, Graham J, Omar MM, Heer R *et al*. Epigenetic inactivation of the human sprouty2 (hSPRY2) homologue in prostate cancer. *Oncogene* 2005; **24**: 2166–2174.
- Fritzsche S, Kenzelmann M, Hoffmann MJ, Muller M, Engers R, Grone HJ *et al*. Concomitant down-regulation of SPRY1 and SPRY2 in prostate carcinoma. *Endocr Relat Cancer* 2006; **13**: 839–849.
- Frank MJ, Dawson DW, Bensinger SJ, Hong JS, Knosp WM, Xu L *et al*. Expression of sprouty2 inhibits B-cell proliferation and is epigenetically silenced in mouse and human B-cell lymphomas. *Blood* 2009; **113**: 2478–2487.
- Fong CW, Chua MS, McKie AB, Ling SH, Mason V, Li R *et al*. Sprouty 2, an inhibitor of mitogen-activated protein kinase signaling, is down-regulated in hepatocellular carcinoma. *Cancer Res* 2006; **66**: 2048–2058.
- Velasco A, Pallares J, Santacana M, Gatiús S, Fernandez M, Domingo M *et al*. Promoter hypermethylation and expression of sprouty 2 in endometrial carcinoma. *Hum Pathol* 2010; **42**: 185–193.
- Macià A, Gallel P, Vaquero M, Gou-Fabregas M, Santacana M, Maliszewska A *et al*. Sprouty1 is a candidate tumor-suppressor gene in medullary thyroid carcinoma. *Oncogene* 2012; **31**: 3961–3972.
- Zheng RQ, Abney E, Chu CQ, Field M, Grubeck-Loebenstien B, Maini RN *et al*. Detection of interleukin-6 and interleukin-1 production in human thyroid epithelial cells by non-radioactive *in situ* hybridization and immunohistochemical methods. *Clin Exp Immunol* 1991; **83**: 314–319.
- Weetman AP, Tandon N, Morgan BP. Antithyroid drugs and release of inflammatory mediators by complement-attacked thyroid cells. *Lancet* 1992; **340**: 633–636.
- Couto JP, Daly L, Almeida A, Knauf JA, Fagin JA, Sobrinho-Simões M *et al*. STAT3 negatively regulates thyroid tumorigenesis. *Proc Natl Acad Sci USA* 2012; **109**: E2361–E2370.
- Kuilman T, Peeper DS. Senescence-messaging secretome: SMS-ing cellular cancer. *Nat Rev Cancer* 2009; **9**: 81–94.
- Tchkonia T, Zhu Y, van Deursen J, Campisi J, Kirkland JL. Cellular senescence and the senescent secretory phenotype: therapeutic opportunities. *J Clin Invest* 2013; **123**: 966–972.
- Acosta JC, Gil J. Senescence: a new weapon for cancer therapy. *Trends Cell Biol* 2012; **22**: 211–219.
- Freund A, Orjalo AV, Desprez PY, Campisi J. Inflammatory networks during cellular senescence: causes and consequences. *Trends Mol Med* 2010; **16**: 238–246.
- Acosta JC, O'Loughlin A, Banito A, Raguz S, Gil J. Control of senescence by CXCR2 and its ligands. *Cell Cycle* 2008; **7**: 2956–2959.
- Kuilman T, Michaloglou C, Vredeveld LC, Douma S, van Doorn R, Desmet CJ *et al*. Oncogene-induced senescence relayed by an interleukin-dependent inflammatory network. *Cell* 2008; **133**: 1019–1031.
- Coppé JP, Patil CK, Rodier F, Sun Y, Muñoz DP, Goldstein J *et al*. Senescence-associated secretory phenotypes reveal cell-nonautonomous functions of oncogenic RAS and the p53 tumor suppressor. *PLoS Biol* 2008; **6**: 2853–2868.
- Wajapeyee N, Serra RW, Zhu X, Mahalingam M, Green MR. Oncogenic BRAF induces senescence and apoptosis through pathways mediated by the secreted protein IGFBP7. *Cell* 2008; **132**: 363–374.
- Acosta JC, O'Loughlin A, Banito A, Gujarró MV, Augert A, Raguz S *et al*. Chemokine signaling via the CXCR2 receptor reinforces senescence. *Cell* 2008; **133**: 1006–1018.
- Orjalo AV, Bhaumik D, Gengler BK, Scott GK, Campisi J. Cell surface-bound IL-1 $\alpha$  is an upstream regulator of the senescence-associated IL-6/IL-8 cytokine network. *Proc Natl Acad Sci USA* 2009; **106**: 17031–17036.
- Chien Y, Scoppo C, Wang X, Fang X, Balgley B, Bolden JE *et al*. Control of the senescence-associated secretory phenotype by NF- $\kappa$ B promotes senescence and enhances chemosensitivity. *Genes Dev* 2011; **25**: 2125–2136.
- Jing H, Kase J, Dörr JR, Milanovic M, Lenze D, Grau M *et al*. Opposing roles of NF- $\kappa$ B in anti-cancer treatment outcome unveiled by cross-species investigations. *Genes Dev* 2011; **25**: 2137–2146.
- Rovillain E, Mansfield L, Caetano C, Alvarez-Fernandez M, Caballero OL, Medema RH *et al*. Activation of nuclear factor-kappa B signaling promotes cellular senescence. *Oncogene* 2011; **30**: 2356–2366.
- Di Cristofano A, Pesce B, Cordon-Cardo C, Pandolfi PP. Pten is essential for embryonic development and tumour suppression. *Nat Genet* 1998; **19**: 348–355.
- Podsypanina K, Ellenson LH, Nemes A, Gu J, Tamura M, Yamada KM *et al*. Mutation of Pten/Mmac1 in mice causes neoplasia in multiple organ systems. *Proc Natl Acad Sci USA* 1999; **96**: 1563–1568.
- Bayascas JR, Leslie NR, Parsons R, Fleming S, Alessi DR. Hypomorphic mutation of PDK1 suppresses tumorigenesis in PTEN (+/–) mice. *Curr Biol* 2005; **15**: 1839–1846.
- Chen Z, Trotman LC, Shaffer D, Lin HK, Dotan ZA, Niki M *et al*. Crucial role of p53-dependent cellular senescence in suppression of Pten-deficient tumorigenesis. *Nature* 2005; **436**: 725–730.
- Alimonti A, Nardella C, Chen Z, Clohessy JG, Carracedo A, Trotman LC *et al*. A novel type of cellular senescence that can be enhanced in mouse models and human tumor xenografts to suppress prostate tumorigenesis. *J Clin Invest* 2010; **120**: 681–693.
- de la Iglesia N, Konopka G, Puram SV, Chan JA, Bachoo RM, You MJ *et al*. Identification of a PTEN-regulated STAT3 brain tumor suppressor pathway. *Genes Dev* 2008; **22**: 449–462.

31. Bowman T, Garcia R, Turkson J, Jove R. STATs in oncogenesis. *Oncogene* 2000; **19**: 2474–2488.
32. Smithgall TE, Briggs SD, Schreiner S, Lerner EC, Cheng H, Wilson MB. Control of myeloid differentiation and survival by Stats. *Oncogene* 2000; **19**: 2612–2618.
33. Bromberg JF, Wrzeszczynska MH, Devgan G, Zhao Y, Pestell RG, Albanese C *et al*. Stat3 as an oncogene. *Cell* 1999; **98**: 295–303.
34. Pectasides E, Egloff AM, Sasaki C, Kountourakis P, Burtneß B, Fountzilias G *et al*. Nuclear localization of signal transducer and activator of transcription 3 in head and neck squamous cell carcinoma is associated with a better prognosis. *Clin Cancer Res* 2010; **16**: 2427–2434.
35. Kim WG, Choi HJ, Kim WB, Kim EY, Yim JH, Kim TY *et al*. Basal STAT3 activities are negatively correlated with tumor size in papillary thyroid carcinomas. *J Endocrinol Invest* 2012; **35**: 413–418.
36. Schneller D, Machat G, Sousek A, Proell V, van Zijl F, Zulehner G *et al*. p19(ARF) / p14(ARF) controls oncogenic functions of signal transducer and activator of transcription 3 in hepatocellular carcinoma. *Hepatology* 2011; **54**: 164–172.
37. Musteanu M, Blaas L, Mair M, Schleder M, Bilban M, Tauber S *et al*. Stat3 is a negative regulator of intestinal tumor progression in Apc(Min) mice. *Gastroenterology* 2010; **138**: 1003–1011; e1001–e1005.
38. Dolled-Filhart M, Camp RL, Kowalski DP, Smith BL, Rimm DL. Tissue microarray analysis of signal transducers and activators of transcription 3 (Stat3) and phospho-Stat3 (Tyr705) in node-negative breast cancer shows nuclear localization is associated with a better prognosis. *Clin Cancer Res* 2003; **9**: 594–600.
39. Michaloglou C, Vredeveld LC, Soengas MS, Denoyelle C, Kuilman T, van der Horst CM *et al*. BRAF600-associated senescence-like cell cycle arrest of human naevi. *Nature* 2005; **436**: 720–724.
40. Dimri GP, Lee X, Basile G, Acosta M, Scott G, Roskelley C *et al*. A biomarker that identifies senescent human cells in culture and in aging skin *in vivo*. *Proc Natl Acad Sci USA* 1995; **92**: 9363–9367.
41. Campisi J. Senescent cells, tumor suppression, and organismal aging: good citizens, bad neighbors. *Cell* 2005; **120**: 513–522.
42. Jayapalan JC, Ferreira M, Sedivy JM, Herbig U. Accumulation of senescent cells in mitotic tissue of aging primates. *Mech Ageing Dev* 2007; **128**: 36–44.
43. Dumont JE, Lamy F, Roger P, Maenhaut C. Physiological and pathological regulation of thyroid cell proliferation and differentiation by thyrotropin and other factors. *Physiol Rev* 1992; **72**: 667–697.
44. Salminen A, Kauppinen A, Kaamiranta K. Emerging role of NF- $\kappa$ B signaling in the induction of senescence-associated secretory phenotype (SASP). *Cell Signal* 2012; **24**: 835–845.
45. Burgess DJ. Senescence. NF- $\kappa$ B shows its beneficial side. *Nat Rev Cancer* 2011; **11**: 832–833.
46. Chiou SH, Shahi P, Wagner RT, Hu H, Lapteva N, Seethammagari M *et al*. The E3 ligase c-Cbl regulates dendritic cell activation. *EMBO Rep* 2011; **12**: 971–979.
47. Kometani K, Yamada T, Sasaki Y, Yokosuka T, Saito T, Rajewsky K *et al*. CIN85 drives B cell responses by linking BCR signals to the canonical NF-kappaB pathway. *J Exp Med* 2011; **208**: 1447–1457.
48. Liu J, Suresh Kumar KG, Yu D, Molton SA, McMahon M, Herlyn M *et al*. Oncogenic BRAF regulates beta-Trcp expression and NF-kappaB activity in human melanoma cells. *Oncogene* 2007; **26**: 1954–1958.
49. Zaremba A, Schmoecker U, Esche H. Sprouty is a cytoplasmic target of adenoviral E1A oncoproteins to regulate the receptor tyrosine kinase signalling pathway. *Virology* 2011; **8**: 192.
50. Litovchick L, Florens LA, Swanson SK, Washburn MP, DeCaprio JA. DYRK1A protein kinase promotes quiescence and senescence through DREAM complex assembly. *Genes Dev* 2011; **25**: 801–813.
51. Schutzman JL, Martin GR. Sprouty genes function in suppression of prostate tumorigenesis. *Proc Natl Acad Sci USA* 2012; **109**: 20023–20028.
52. Patel R, Gao M, Ahmad I, Fleming J, Singh LB, Rai TS *et al*. Sprouty2, PTEN, and PP2A interact to regulate prostate cancer progression. *J Clin Invest* 2013; **123**: 1157–1175.
53. Prieur A, Peeper DS. Cellular senescence *in vivo*: a barrier to tumorigenesis. *Curr Opin Cell Biol* 2008; **20**: 150–155.
54. Collado M, Serrano M. Senescence in tumours: evidence from mice and humans. *Nat Rev Cancer* 2010; **10**: 51–57.
55. Basolo F, Fiore L, Pollina L, Fontanini G, Conaldi PG, Toniolo A. Reduced expression of interleukin 6 in undifferentiated thyroid carcinoma: *in vitro* and *in vivo* studies. *Clin Cancer Res* 1998; **4**: 381–387.
56. Vizioli MG, Sensi M, Miranda C, Cleris L, Formelli F, Anania MC *et al*. IGFBP7: an oncosuppressor gene in thyroid carcinogenesis. *Oncogene* 2010; **29**: 3835–3844.
57. Rodríguez-Rodero S, Fernández AF, Fernández-Morera JL, Castro-Santos P, Bayon GF, Ferrero C *et al*. DNA methylation signatures identify biologically distinct thyroid cancer subtypes. *J Clin Endocrinol Metab* 2013; **98**: 2811–2821.
58. Courtois-Cox S, Genter Williams SM, Reczek EE, Johnson BW, McGillicuddy LT, Johannessen CM *et al*. A negative feedback signaling network underlies oncogene-induced senescence. *Cancer Cell* 2006; **10**: 459–472.
59. Hall JA, Ribich S, Christoffolete MA, Simovic G, Correa-Medina M, Patti ME *et al*. Absence of thyroid hormone activation during development underlies a permanent defect in adaptive thermogenesis. *Endocrinology* 2010; **151**: 4573–4582.
60. Encinas M, Rozen EJ, Dolcet X, Jain S, Comella JX, Milbrandt J *et al*. Analysis of Ret knockin mice reveals a critical role for IKKs, but not PI 3-K, in neurotrophic factor-induced survival of sympathetic neurons. *Cell Death Differ* 2008; **15**: 1510–1521.

Supplementary Information accompanies this paper on Cell Death and Differentiation website (<http://www.nature.com/cdd>)